

# Autogenous shrinkage of concrete containing granulated blast-furnace slag

K.M. Lee <sup>a</sup>, H.K. Lee <sup>b,\*</sup>, S.H. Lee <sup>b</sup>, G.Y. Kim <sup>c</sup>

<sup>a</sup> *Department of Civil and Environmental Engineering, Sungkyunkwan University, Suwon, Korea*

<sup>b</sup> *Research Institute of Technology, Samsung Construction and Engineering, Sungnam, Korea*

<sup>c</sup> *Division of Architecture, Chungnam National University, Daejeon, Korea*

Received 19 July 2005; accepted 12 January 2006

## Abstract

This paper presents the experimental results and prediction model for the autogenous shrinkage of concrete made with various water-to-cementitious materials ratios ( $w/cm$ ) ranging from 0.27 to 0.42 and granulated blast-furnace slag (BFS) in the range of 0% to 50% by mass of the total cementitious materials. Test results showed that BFS concrete exhibited greater autogenous shrinkage than ordinary concrete with no BFS with the same  $w/cm$ , and that the higher the BFS content, the greater the autogenous shrinkage. At the same content of BFS, the increasing rate of autogenous shrinkage is affected by the  $w/cm$ ; the lower the  $w/cm$ , the smaller the increasing rate of autogenous shrinkage. Based on the test results, a prediction model for autogenous shrinkage was proposed. In particular, an effective autogenous shrinkage that is a realistic shrinkage strain responsible for stress development was introduced in the model. It was determined by taking into account the characteristics of ultrasonic pulse velocity evolution in concrete. This prediction method for autogenous shrinkage may be effectively used to estimate the stress induced by autogenous shrinkage.

© 2006 Elsevier Ltd. All rights reserved.

**Keywords:** Shrinkage; Modeling; Granulated blast-furnace slag; Concrete

## 1. Introduction

In the past decades, great efforts have been made to develop a new generation of concrete to improve its performance and competitiveness as a construction material. As a result, concrete exhibiting high performance and high durability has been developed and is used more frequently to construct civil infrastructures. However, such concrete is more prone to early age cracking caused by autogenous shrinkage due to the use of rather low water-to-cementitious material ratio ( $w/cm$ ) and mineral admixtures such as silica fume.

Early age cracking of concrete results from the interplay between the volume instability, the mechanical properties of concrete and different types and degrees of restraint [1]. When the concrete behaves like a fluid, i.e., during the very early age, its volumetric changes are usually not of a great concern in terms of stress generation because the concrete deforms

plastically without generating stresses. However, once it has transformed a visco-elastic solid, the stress is generated [2]. This transition is very important with respect to the initiation of autogenous shrinkage strain and induced stress.

Determination of the initiation point of autogenous shrinkage is not easy because of the complex fluid–solid transition happening around setting. Thus, it is sometimes difficult to compare the shrinkage results directly because autogenous shrinkage is zeroed at different times, despite plenty of quantitative studies in the literature. Actually, autogenous shrinkage is strongly dependent on the start time of measurement because self-desiccation starts to develop as soon as hydration begins. Therefore, in order to obtain the maximum potential autogenous shrinkage, it must be measured before the specimen has aged 24 h and preferably before initial setting time [3].

A technical committee on autogenous shrinkage at the Japan Concrete Institute (JCI) defined autogenous shrinkage as the macroscopic volume reduction of cementitious materials when cement hydrates after initial setting [4]. This definition implies that the initial setting time is the start point of autogenous shrinkage. However, the setting times, which are measured in

\* Corresponding author.

E-mail address: [hoikeun.lee@samsung.com](mailto:hoikeun.lee@samsung.com) (H.K. Lee).

Table 1  
Physical properties and chemical composition of cement and granulated blast-furnace slag

Materials	Physical properties		Chemical composition (%)						
	Specific gravity	Blaine (m <sup>2</sup> /kg)	SiO <sub>2</sub>	Al <sub>2</sub> O <sub>3</sub>	Fe <sub>2</sub> O <sub>3</sub>	CaO	MgO	SO <sub>3</sub>	LOI
Cement	3.14	320	21.7	5.0	3.3	62.4	2.1	2.4	0.82
Slag	2.94	430	31.6	14.6	0.4	42.4	2.1	3.0	0.02

accordance to the penetration resistance test method (ASTM C 403) are determined somewhat arbitrarily. Furthermore, setting times may not necessarily coincide with the transition, and may not be associated with the characteristic physico-chemical and microstructural changes of concrete [5]. Therefore, an easier and more practical method for monitoring the transition of concrete is needed.

Granulated blast-furnace slag (BFS), either as a constituent of cement or as a mineral admixture, is widely used to make not only traditional concrete but also high-performance concrete, which has several advantages in terms of workability, long-term strength, and durability. BFS has been successfully applied in Korea, particularly in marine concrete structures because of its low permeability and pore refinement. In fact, however, the BFS in concrete further increases autogenous shrinkage [6–8]. The high autogenous shrinkage due to the use of BFS would cause severe cracking in concrete structures. Even if cracking does not seem to occur, there is considerable residual stress within the concrete. Thus, any additional unexpected load, superimposed on the internal residual stress, such as the one induced by thermal gradients or movement of the formwork, can tilt the balance and result in an overall stress greater than the tensile strength of the concrete, and finally, lead to cracking [9]. Therefore, autogenous shrinkage of concrete containing BFS must be estimated accurately. It should be also mitigated to prevent cracking and to improve the quality and service life of concrete structures. Previous research on the autogenous shrinkage in cement paste and in concrete have mostly dealt with the effect of silica fume, so only limited information is currently available on autogenous shrinkage of concrete containing BFS.

This study investigated the effect of  $w/cm$  and BFS percentage on the autogenous shrinkage of concrete, and then a prediction model for autogenous shrinkage was proposed based on the test results. In particular, an estimation formula of the 28-day effective autogenous shrinkage was determined by considering various  $w/cms$  and characteristics of UPV evolution.

## 2. Experimental work

### 2.1. Materials and mixture proportioning of concrete

Type I portland cement and granulated blast-furnace slag (BFS) produced in Korea were used as cementitious materials to prepare the concrete mixtures. Their physical properties and chemical composition are given in Table 1. The fine and coarse aggregates were washed river sand with specific gravity of 2.58, water absorption of 1.03%, fineness modulus of 2.86, and crushed granite with specific gravity of 2.62 and maximum-size of 25 mm, respectively.

Table 2 shows the mixture proportioning of twelve concrete mixtures evaluated in this study. All concrete mixtures had the same unit water content of 168 kg, while the corresponding unit content of cementitious materials was increased from 400 to 622 kg as the  $w/cm$  was decreased. This means that the paste content by volume is lower in the high- $w/cm$  concrete mixtures, which implies that it can influence on the autogenous shrinkage because the coarse aggregate restrain the shrinkage deformation proportionally to its volume ratio and stiffness. It should be noted here that the effort is undertaken to evaluate the autogenous deformation of concrete mixtures with the same unit water content.

Concrete mixtures without any BFS were designated as OPC concrete, whereas the other made with BFS were designated as BFS30 and BFS50 concretes, where the numerical notation after 'BFS' corresponds to the replacement percentage of BFS. A naphthalene-based high-range water-reducing admixture (HRWRA) with a dark brown solution and air-entraining admixture (AEA) were used to adjust the slump value of  $180 \pm 20$  mm and air content in all mixtures.

Table 2  
Mixture proportioning of concrete per cubic meter

$w/cm$	Replacement % of BFS	Codification	Water (kg)	Type I cement (kg)	BFS (kg)	Sand (kg)	Coarse agg. (kg)	AEA (cm <sup>3</sup> × wt. %)	HRWRA (cm × wt. %)
0.42	0	42-OPC	168	400	0	783	972	0.015	0.70
	30	42-BFS30	168	280	120	780	968	0.013	0.45
	50	42-BFS50	168	200	200	778	966	0.013	0.40
0.37	0	37-OPC	168	454	0	729	981	0.017	0.80
	30	37-BFS30	168	318	136	726	977	0.015	0.50
	50	37-BFS50	168	227	227	724	974	0.015	0.45
0.32	0	32-OPC	168	525	0	672	981	0.018	1.00
	30	32-BFS30	168	368	157	668	976	0.018	0.85
	50	32-BFS50	168	263	262	665	972	0.017	0.75
0.27	0	27-OPC	168	622	0	608	965	0.020	1.50
	30	27-BFS30	168	435	187	604	959	0.020	1.35
	50	27-BFS50	168	311	311	601	954	0.020	1.25

<sup>a</sup> Cementitious materials = Cement + BFS.

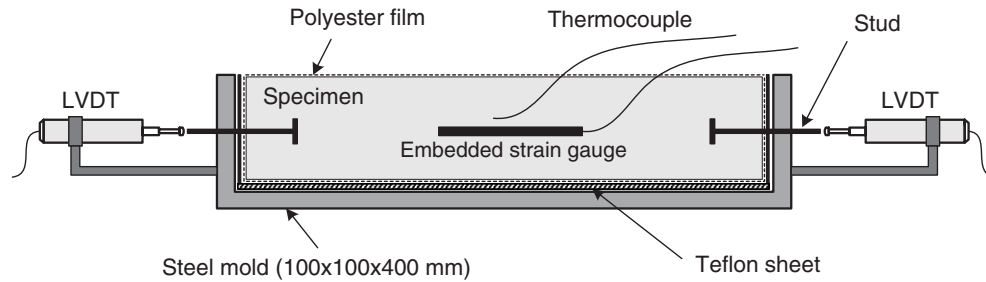


Fig. 1. Experimental set-up for measuring any change in the length of the concrete before demolding.

## 2.2. Specimen preparation and test method

### 2.2.1. Free autogenous shrinkage

In order to measure the length change of concrete at early age, the method similar to the one proposed by Japan Concrete Institute (JCI) was used, as shown in Fig. 1. For each mixture, two concrete prisms of  $100 \times 100 \times 400$  mm were prepared. Before the removal of the mold, two LVDTs contacted on the stud and an embedded strain gauge measuring 120-mm in length positioned at the center of the specimen were installed to monitor the length change of the specimen. Immediately after demolding at 24 h, the specimens were sealed with an adhesive aluminum tape to avoid moisture loss, and any change in the length was recorded by the embedded strain gauge only. All specimens were stored in a chamber at a  $20 \pm 1$  °C and a relative humidity of  $60 \pm 3\%$  during the test. The first measurement of length change in sample was carried out at 3 h after cement contact with water.

Autogenous shrinkage can be influenced by the thermal expansion and contraction caused by the temperature change in concrete due to hydration reaction. Therefore, a thermocouple was cast to monitor the temperature variations in each specimen. The measurement of autogenous shrinkage was corrected for thermal strain by assuming that the linear thermal expansion coefficient of concrete was  $10 \times 10^{-6}/^{\circ}\text{C}$ .

### 2.2.2. Monitoring of ultrasonic pulse velocity

An ultrasonic monitoring system, which can measure the longitudinal ultrasonic pulse velocity (UPV) at any desired intervals, was constructed and it is detailed in Ref. [10]. Fresh mixture was poured in the container and properly compacted. The UPV measurement started 3 h and continued for 24 h at 30-min intervals. The UPV can be easily calculated by dividing the length of the straight wave path through the sample by the travel time of the ultrasonic pulse. All UPV measurements at the laboratory were conducted at the same condition of autogenous shrinkage measurement.

## 3. Results and discussion

### 3.1. Properties of fresh and hardened concrete

Table 3 shows the slump, air content, and compressive strength of concrete evaluated at given ages, measured in accordance to ASTM C 143, C 231, and C 39, respectively. The

slump value of the tested mixtures was  $180 \pm 20$  mm, and air content varied from 1.5% to 5.6%. Table 3 revealed that by 3 days, compressive strength of all concrete made with BFS was lower than that of OPC concrete. After 28 days of curing in water, however, BFS concrete exhibited similar or slightly higher compressive strength than the OPC concrete with the same  $w/cm$ .

### 3.2. Free autogenous shrinkage

Fig. 2 shows the free autogenous shrinkage strain of the tested concrete up to 180 days. In the figures, the solid lines represent the predicted value obtained from a proposed model. The value will be discussed in the next section.

All BFS concrete had higher autogenous shrinkage than the OPC concretes with the same  $w/cm$ , and the higher the BFS replacement percentage, the higher the autogenous shrinkage. This result is in agreement with those reported by previous researches [6–8]. At 28 days, when  $w/cm$  was 0.37 or 0.42, the autogenous shrinkage of BFS30 and BFS50 were increased by about 31–56% and 58–76%, respectively, compared with that of OPC with the same  $w/cm$ . However, the mixture made with  $w/cm$  of 0.27 exhibited relatively small increase of autogenous shrinkage; 6.6% for BFS30 and 17.4% for BFS50 at 28 days. The higher autogenous shrinkage of concrete containing BFS may be due to the greater chemical shrinkage than that of the concrete with pure portland cement. Thus, the greater shrinkage led to faster and greater self-desiccation, and resulted in larger

Table 3  
Initial slump, air content, and compressive strength of concrete

Codification	Slump (mm)	Air content (%)	Compressive strength (MPa)					
			1 day	3 days	7 days	28 days	90 days	180 days
42-OPC	180	4.7	17.0	29.8	37.2	46.1	50.8	55.3
42-BFS30	180	4.8	5.1	19.5	30.2	44.9	51.7	53.1
42-BFS50	190	5.6	2.4	14.8	27.3	44.6	52.3	54.3
37-OPC	180	3.8	19.6	36.1	42.3	50.5	53.8	60.7
37-BFS30	180	4.2	10.3	27.2	39.2	56.3	57.8	60.8
37-BFS50	160	3.7	5.2	22.2	35.7	57.1	58.6	61.9
32-OPC	180	2.1	30.4	39.3	55.0	60.0	70.6	73.8
32-BFS30	190	1.8	11.8	40.5	57.4	64.3	74.5	75.2
32-BFS50	200	2.8	10.0	35.4	54.9	66.7	74.9	75.3
27-OPC	180	2.2	31.1	54.4	63.3	71.4	80.7	85.3
27-BFS30	190	1.5	–	52.7	70.3	72.6	83.9	86.5
27-BFS50	200	1.7	–	46.2	69.2	76.2	86.2	89.6

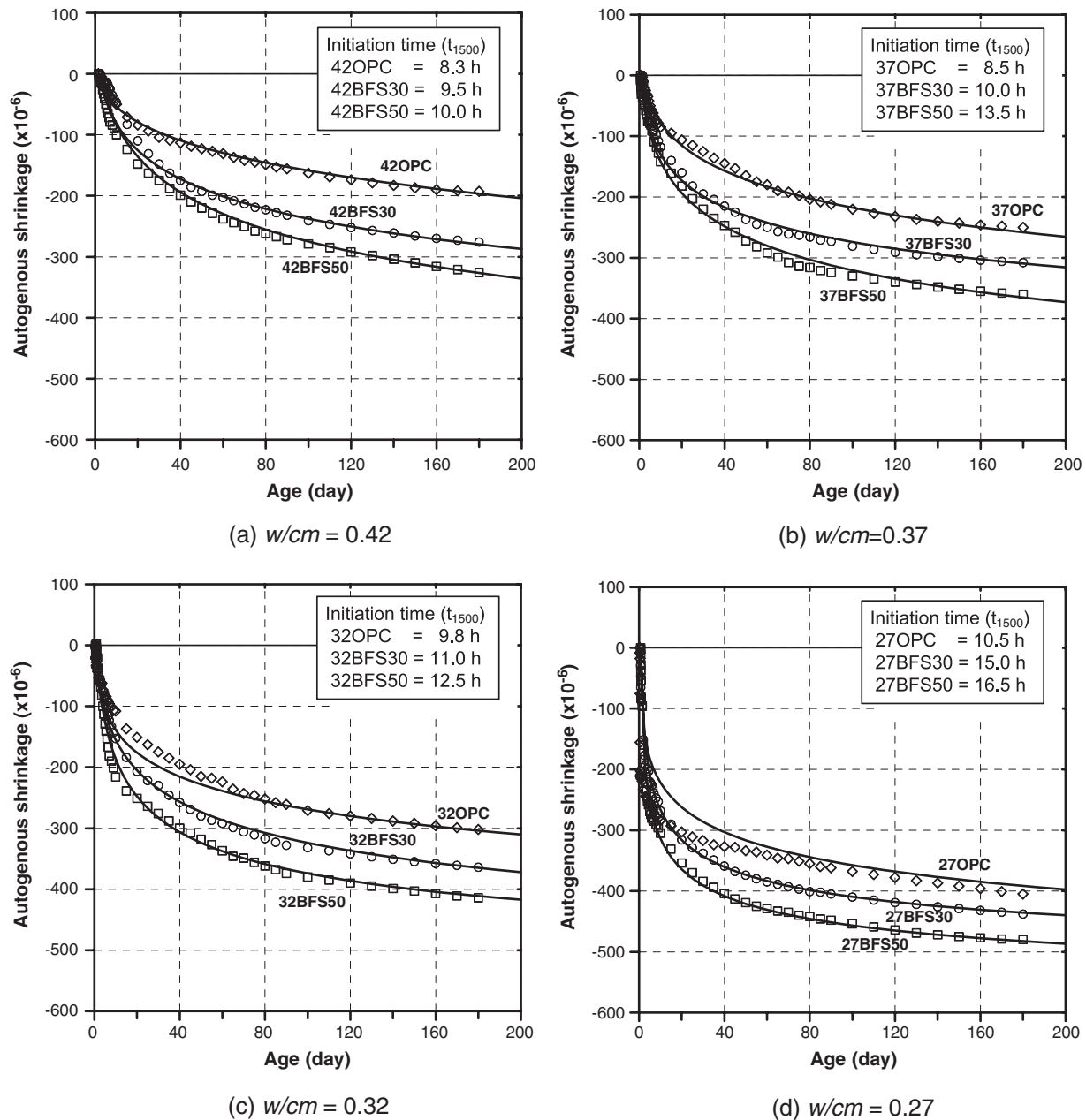


Fig. 2. Experimental results and predicted values for autogenous shrinkage of concrete containing granulated blast-furnace slag with various  $w/cm$ s.

autogenous shrinkage [11]. Moreover, the use of BFS makes a cement paste have a finer pore structure, as confirmed by permeability [12]. Finer pores contribute to a lower relative humidity, which increases the degree of self-desiccation within the cement paste.

Table 4 lists the autogenous shrinkage strain for each concrete evaluated at 3, 7, 28, and 180 days of age. The value in parenthesis represents the ratio of the autogenous shrinkage strain at given ages to the 180-day autogenous shrinkage strain. The low- $w/cm$  concrete experienced autogenous shrinkage faster than the high- $w/cm$  concrete regardless of the concrete type. For the concrete mixtures with  $w/cm$  of 0.27 (27-OPC, 27-BFS30, and 27-BFS50), about 54% or more of the autogenous shrinkage up to 180 days occurred at 7 days of age,

while for the concrete made with  $w/cm$  of 0.37 (37-OPC, 37-BFS30, and 37-BFS50) only 27–30% occurred during the same period.

### 3.3. Relationship between UPV evolution and autogenous shrinkage

As mentioned earlier in the Introduction, it is important to know the transition time of a given concrete because it is related to the stress generation. One possible method for evaluating the transition of concrete is to use an ultrasonic technique, with which depending on the age of the concrete, amplitude-, velocity-, and frequency-variations can be observed during the transition from viscous suspension to plastic state of the mixture [10].

Table 4

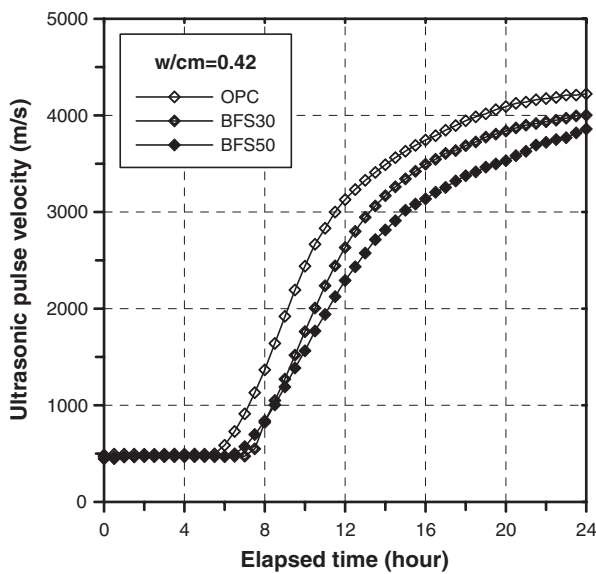
Free autogenous shrinkage strain of concrete evaluated at specified ages

w/cm	Autogenous shrinkage strain ( $\times 10^{-6}$ ) (% of 180-day shrinkage)											
	OPC				BFS30				BFS50			
	3 days	7 days	28 days	180 days	3 days	7 days	28 days	180 days	3 days	7 days	28 days	180 days
0.27	244 (60) <sup>a</sup>	271 (67)	317 (78)	405 (100)	193 (44)	239 (54)	338 (77)	438 (100)	216 (45)	285 (59)	384 (80)	480 (100)
0.32	64 (21)	96 (32)	175 (58)	302 (100)	62 (17)	123 (34)	230 (63)	364 (100)	69 (17)	181 (44)	276 (67)	414 (100)
0.37	25 (9)	68 (27)	125 (50)	250 (100)	36 (12)	90 (29)	195 (63)	308 (100)	58 (16)	109 (30)	220 (61)	360 (100)
0.42	19 (10)	37 (19)	104 (54)	193 (100)	6 (2)	25 (9)	148 (54)	276 (100)	16 (5)	79 (24)	175 (54)	326 (100)

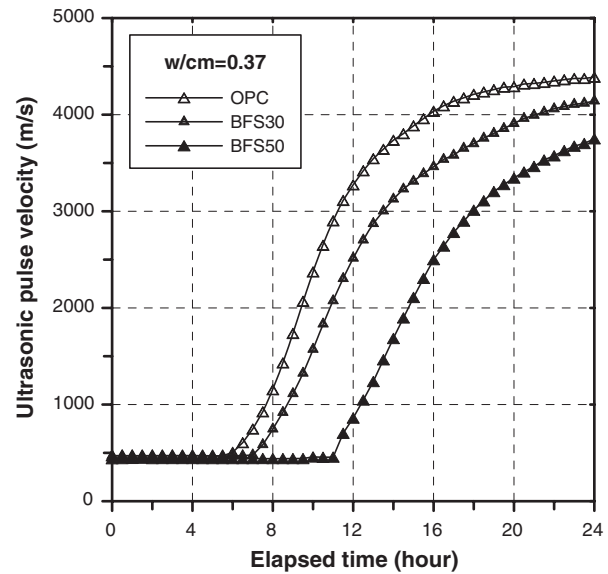
<sup>a</sup> Ratio of autogenous shrinkage strain at 3, 7, and 28 days to the 180-day autogenous shrinkage strain.

Fig. 3 compares the evolution of the UPV monitored over the first 24 h for all concrete mixtures made with BFS replacement percentage of 0%, 30%, and 50% at the same w/cm. All UPV

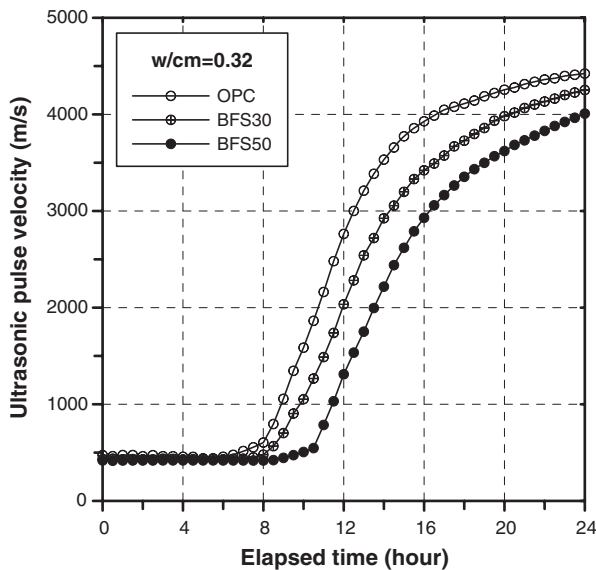
curves shown in Fig. 3 were similar to the curves as observed by other researchers [13–15]. All concrete mixtures had almost the same UPV at very early age regardless of w/cm or BFS content



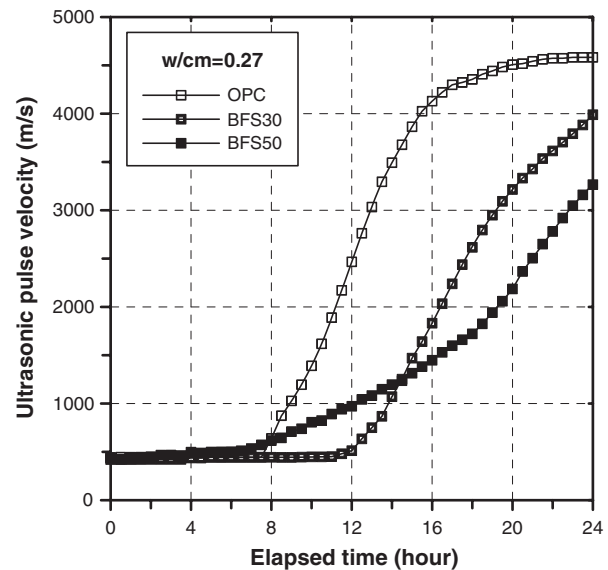
(a) w/cm=0.42



(b) w/cm = 0.37



(c) w/cm = 0.32



(d) w/cm = 0.27

Fig. 3. Evolution of UPV of concrete with the BFS replacement level of 0%, 30%, and 50%.



(400–500 m/s). Afterward, the UPV started to increase as the hydration continued at different rates. In particular, the mixture made with a relatively low  $w/cm$  of 0.27 and BFS replacement level of 50% (Fig. 3(d)) had different evolution trend of UPV compared to other mixtures, which exhibited gradual and prolonged development of UPV. The possible explanation is that the cement particles in the low  $w/cm$  cases may begin to become connected at relatively early ages because of the relatively short distances between them, but massive hydration is delayed due to the presence of the BFS in addition to the HRWRA effects [10]. The stiffening process of a specific concrete mixture could be investigated by the monitoring of the UPV, which could be used to determine the transition time of concrete.

When the hydrates percolate and the first solid paths are formed in the hardening paste, the stiffness as well as the UPV starts to increase because the wave velocity is directly associated with the stiffness of material. Thus, the time at which the UPV begins to increase has been used as the criterion for transition and would be related to the initial set. However, the time cannot be identified from the UPV curve for every case, particularly when large amount of mineral admixture and/or high dosage of HRWRA, which causes the set retardation, is used for making the concrete [10]. Therefore, in this study, an effective autogenous shrinkage, i.e. a realistic shrinkage strain responsible for stress generation, was defined as the shrinkage that occurred after the UPV reaches a specific value, as defined by Pessiki and Carino [16]. In this study, UPV value of 1500 m/s was suggested as a target velocity for the initiation of autogenous shrinkage because of the following reasons: The wave velocity is proportional to the square root of the stiffness (or elastic modulus) of a material. By assuming that the UPV of concrete at 28 days is about 4500 m/s, as shown in Fig. 3, the stiffness becomes one-ninth of the 28-day stiffness, where the UPV equals to 1500 m/s. Consequently, the stress generated at

Table 5

Coefficient,  $\gamma$  in Eq. (1) and constant,  $a$  and  $b$ , in Eq. (3)

Codification	$w/cm$	$\gamma$	$a$	$b$
42-OPC	0.42	1.00	3.365	0.132
42-BFS30		1.59	1.565	0.272
42-BFS50		1.88	1.491	0.307
37-OPC	0.37	1.00	1.708	0.258
37-BFS30		1.44	1.215	0.253
37-BFS50		1.63	1.208	0.290
32-OPC	0.32	1.00	1.413	0.201
32-BFS30		1.18	1.115	0.285
32-BFS50		1.42	0.753	0.397
27-OPC	0.27	1.00	1.121	0.185
27-BFS30		1.20	0.516	0.358
27-BFS50		1.37	0.466	0.344

that time would be negligible not only because of the relatively low stiffness, but also stress relaxation. Moreover, comparing the setting times obtained from penetration resistance test method and the corresponding UPV evolution curve, it was found that the initial setting time was not the same as the time at which the UPV started to increase. The setting occurred after a few hours when the UPV began to increase, and the corresponding UPV was roughly 1500 m/s [10]. Of course, the setting times or the increasing time of UPV does not have to be used as the indication time of the initiation of autogenous shrinkage. However, a specified UPV value would be simpler and easier to apply in practice.

### 3.4. Prediction model for autogenous shrinkage

Several researchers have tried to predict autogenous shrinkage [17–20]. In this study, the following prediction model that considers an effective autogenous shrinkage at 28 days was adopted [21].

$$\varepsilon_{as}(t) = \gamma \varepsilon_{28}(w/cm) \cdot \beta(t) \quad (1)$$

$$\varepsilon_{28} = 2080 \exp[-7.4(w/cm)] \quad (2)$$

$$\beta(t) = \exp \left\{ a \left[ 1 - \left( \frac{28 - t_{1500}}{t - t_{1500}} \right)^b \right] \right\} \quad (3)$$

where,

- $\varepsilon_{as}(t)$  autogenous shrinkage strain ( $\times 10^{-6}$ )
- $\varepsilon_{28}$  autogenous shrinkage strain at 28 days ( $\times 10^{-6}$ )
- $\gamma$  coefficient to describe to the effect of BFS
- $t_{1500}$  time at which the UPV reaches 1500 m/s (day)
- $a, b$  constants that depend on the replacement level of BFS
- $t$  age of concrete (day).

In order to compare the  $\varepsilon_{28}$  according to the start time of autogenous shrinkage, three criteria, i.e., initial and final setting time, and  $t_{1500}$ , were considered. Fig. 4 is a plot of the  $w/cm$  versus the corresponding the 28-day effective autogenous shrinkage strain for OPC concrete. In the figure, solid and dashed lines represent the fitted curve obtained by regression

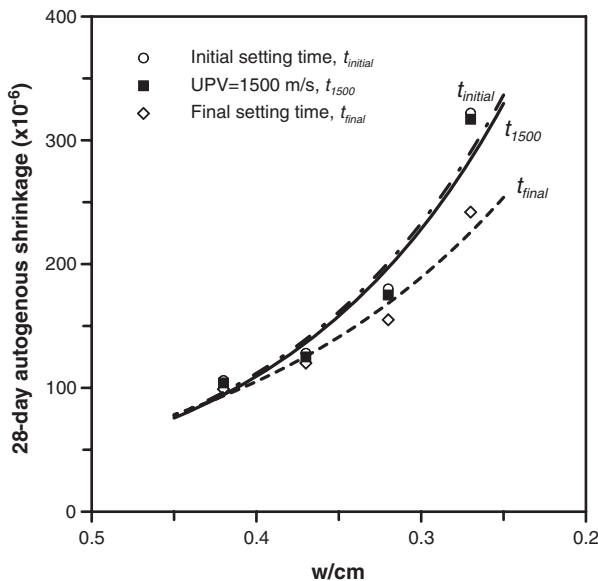


Fig. 4. Relationship between the  $w/cm$  of OPC concrete and its 28-day effective autogenous shrinkage strain depending on the three criteria.

analysis. Two curves for  $t_{1500}$  and initial setting time showed a similar trend, while that of the final setting time exhibited a different trend, as  $w/cm$  decreased. Also, an exponential relation was suitable for the data.

By applying the test data to the autogenous shrinkage model in Eq. (1), coefficient  $\gamma$  and constants,  $a$  and  $b$ , were determined, as given in Table 5.  $\gamma$  of BFS concrete were greater than 1.0 and increased with increasing the BFS replacement level at the same  $w/cm$ , implying that the presence of BFS increases the autogenous shrinkage. At the same replacement level of BFS,  $\gamma$  was gradually decreased with decreasing the  $w/cm$ . In other words, when the replacement level of BFS was the same, BFS effects on autogenous shrinkage varied according to the  $w/cm$ . At the same  $w/cm$  and higher replacement level of BFS,  $a$  decreased with decreasing the  $w/cm$  while  $b$  increased. For the same concrete,  $a$  decreased as the  $w/cm$  decreased while  $b$  did not show the consistent trend.

As shown in Fig. 2, little difference between measured autogenous shrinkage results and predicted results can be observed. In particular, relatively large discrepancy was obtained for the 32-OPC and 27-OPC mixture, particularly before and after 28 days. This is attributed to the difference between the measured autogenous shrinkage at 28 days and predicted one by Eq. (2). Therefore, more data on the 28-day autogenous shrinkage are needed to improve the accuracy of prediction.

#### 4. Conclusions

The autogenous shrinkage of concrete made with  $w/cm$  ranging from 0.27 to 0.42 and BFS replacement level of 0%, 30%, and 50% was evaluated. The concrete made with BFS exhibited higher autogenous shrinkage than ordinary concrete without any BFS, and the higher the BFS replacement level, the greater the autogenous shrinkage at the same  $w/cm$ . This may be due to the greater chemical shrinkage and finer pore structure of the concrete with BFS than pure portland cement, and the particle shape of BFS.

Based on the limited experimental results, a prediction model for autogenous shrinkage, including the effect of  $w/cm$  and BFS, was proposed. In particular, the start time of autogenous shrinkage was determined by ultrasonic test, and then an effective autogenous shrinkage can be predicted by the model. BFS in concrete could increase autogenous shrinkage, thus a method to reduce autogenous shrinkage and induced stress must be investigated.

#### Acknowledgments

The authors wish to acknowledge the financial support of the Ministry of Construction and Transportation through the Korea Bridge Design and Engineering Research Center and Samsung Corporation Co., Ltd.

#### References

- [1] A. Radocea, Autogenous volume change of concrete at very early-age, *Mag. Concr. Res.* 50 (1998) 107–113.
- [2] A. Bentur, Comprehensive approach to prediction and control of early-age cracking in cementitious materials, in: F.-J. Ulm, Z.P. Bazant, F.H. Wittmann (Eds.), *Creep, Shrinkage and Durability Mechanics of Concrete and Other Quasi-Brittle Materials*, Proc. of Sixth Int. Conf., Elsevier Science Ltd., 2001, pp. 589–598.
- [3] P.-C. Aïtcin, Demystifying autogenous shrinkage, *Concr. Int.* 21 (1999) 54–56.
- [4] Japan Concrete Institute, in: Tazawa (Ed.), *Technical Committee Report on Autogenous Shrinkage*, Proc. of Int. Workshop, E&FN Spon, London, 1998, pp. 1–63.
- [5] P.K. Mehta, J.M. Monteiro, *Concrete: Structure, Properties, and Materials*, 2nd edition, Prentice Hall, New Jersey, 1993.
- [6] E. Tazawa, S. Miyazawa, Influence of cement and admixture on autogenous shrinkage of cement paste, *Cem. Concr. Res.* 25 (1995) 281–287.
- [7] S.N. Lim, T.H. Wee, Autogenous shrinkage of ground-granulated blast-furnace slag concrete, *ACI Mater. J.* 97 (2000) 587–593.
- [8] P. Lura, K. Breugel, I. Maruyama, Effect of curing temperature and type of cement on early-age shrinkage of high-performance concrete, *Cem. Concr. Res.* 31 (2001) 1867–1872.
- [9] A. Bentur, Early-age shrinkage and cracking in cementitious systems, in: V. Baroghel-Bouny, P.-C. Aïtcin (Eds.), *Proc. of International RILEM Workshop on Shrinkage of Concrete*, Shrinkage 2000, RILEM, Paris, France, 2000, pp. 1–20.
- [10] H.K. Lee, K.M. Lee, Y.H. Kim, H. Yim, D.B. Bae, Ultrasonic in-situ monitoring of setting process of high-performance concrete, *Cem. Concr. Res.* 34 (2004) 631–640.
- [11] P. Lura, Autogenous deformation and internal curing of concrete. PhD Thesis, Delft University of Technology, Delft, 2003.
- [12] D.M. Roy, G.M. Idorn, Hydration, structure and properties of blast-furnace slag cements, mortars, and concrete, *ACI J.* 79 (1982) 444–457.
- [13] J. Keating, D.J. Hannant, A.P. Hibbert, Correlation between cube strength, ultrasonic pulse velocity and volume change for oil well cement slurries, *Cem. Concr. Res.* 19 (1989) 715–726.
- [14] S. Popovics, R. Silva-Rodriguez, J.S. Popovics, V. Martucci, Behavior of ultrasonic pulses in fresh concrete, *New Experimental Techniques for Evaluating Concrete Materials and Structural Performance*, SP-143, ACI, 1993, pp. 207–225.
- [15] T. Chotard, N. Gimet-Brert, A. Smith, D. Fargeto, J.P. Bonnet, C. Gault, Application of ultrasonic testing to describe the hydration of calcium aluminate cement at the early age, *Cem. Concr. Res.* 31 (2001) 405–412.
- [16] S.P. Pessiki, N.J. Carino, Setting time and strength of concrete using the impact-echo method, *ACI Mater. J.* 85 (1988) 389–399.
- [17] S. Miyazawa, E. Tazawa, Prediction model for shrinkage of concrete including autogenous shrinkage, in: F.-J. Ulm, Z.P. Bazant, F.H. Wittmann (Eds.), *Creep, Shrinkage and Durability Mechanics of Concrete and Other Quasi-Brittle Materials*, Proc. of Sixth Int. Conf., Elsevier Science Ltd., 2001, pp. 735–746.
- [18] CEB-FIP 2000, *Structural Concrete: Textbook on Behavior, Design and Performance*, vol. 1, Sprint-Druck, Stuttgart, 1999, pp. 43–46.
- [19] J.E. Jonasson, H. Hedlund, An engineering model for creep and shrinkage in HPC, in: V. Baroghel-Bouny, P.-C. Aïtcin (Eds.), *Proc. of International RILEM Workshop on Shrinkage of Concrete*, Shrinkage 2000, RILEM, Paris, France, 2000, pp. 507–529.
- [20] W.H. Dilger, C. Wang, Creep and shrinkage of HPC, in: A. Al-Manaseer (Ed.), *Creep and Shrinkage-Structural Design Effects*, SP-194, American Concrete Institute, Farmington Hills, Michigan, 2000, pp. 361–379.
- [21] H.K. Lee, K.M. Lee, B.K. Kim, Autogenous shrinkage of high-performance concrete containing fly ash, *Mag. Concr. Res.* 55 (2003) 507–515.